

# Renormalization of Quantum Fields on the Lightcone Worldsheet I: Scalar Fields<sup>1</sup>

Charles B. Thorn<sup>2</sup>

*Institute for Fundamental Theory  
Department of Physics, University of Florida, Gainesville FL 32611*

## Abstract

We show that the lightcone worldsheet formalism, constructed to represent the sum of the bare planar diagrams of scalar  $\phi^3$  field theory, survives the renormalization procedure in space-time dimensions  $D \leq 6$ . Specifically this means that all the counter-terms, necessary to produce a successful renormalized perturbation expansion to all orders, can be represented as local terms in the lightcone worldsheet action. Because the worldsheet regulator breaks Lorentz invariance, we find the need for two non-covariant counter-terms, in addition to the usual mass, coupling and wave function renormalization. One of these can be simply interpreted as a rescaling of transverse coordinates with respect to longitudinal coordinates. The second one introduces couplings between the matter and ghost worldsheet fields on the boundaries.

---

<sup>1</sup>Supported in part by the Department of Energy under Grant No. DE-FG02-97ER-41029.

<sup>2</sup>E-mail address: thorn@phys.ufl.edu

# 1 Introduction

The possible duality between string and field theory has been a recent active topic of investigation since Maldacena proposed that IIB superstring theory on an  $\text{AdS}_5 \times \text{S}_5$  background is equivalent to supersymmetric Yang-Mills field theory with extended  $\mathcal{N} = 4$  supersymmetry [1]. The most exciting application of this new string theory technique is, without doubt, the confinement problem of QCD. Most mechanisms proposed to account for quark confinement involve the formation of a color flux tube or gluon chain, and it may well be that formulating QCD as a string theory provide the most tractable realization of such a physical mechanism. Most of the literature on this subject concentrates on how typically field theoretic phenomena are accounted for in a string formulation [2, 3]. The program initiated by Bardakci and me takes the opposite tack, seeking a direct construction of a stringy worldsheet formalism that sums the planar diagrams of quantum field theory [4–6]. These three articles lay the foundations of this “bottom-up” approach: the first sets up a worldsheet formalism for scalar  $\Phi^3$  theory, the second for Yang-Mills theory, and the third for the whole range of interesting supersymmetric Yang-Mills theories, including  $\mathcal{N} = 1, 2, 4$  extended supersymmetry. We note that in the AdS/CFT context, an approach connecting perturbative field theory to string theory on pp-wave backgrounds [7] shares to some extent the spirit and goals of our program, as does Witten’s formulation of perturbative gauge theory as string on twistor space [8].

The worldsheet formalism developed in [4–6] reproduces the multi-loop expansion of the *bare* planar Feynman diagrams, singled out by ’t Hooft’s large  $N_c$  limit [9]. Because the bare diagrams are divergent in interesting space-time dimensions (*i.e.*  $D > 2$ ), the representation must be regarded as formal except when applied to tree diagrams. It is therefore crucial to establish that the worldsheet description survives the renormalization procedure which systematically removes the ultraviolet infinities of quantum field theory. Since the worldsheet formalism sacrifices manifest Lorentz invariance, it is logically possible that counter-terms required to ensure Lorentz invariance after renormalization might not have a local worldsheet interpretation. Such an outcome would significantly diminish the usefulness of the formalism for accessing non-perturbative physics in the field theory. The purpose of this article is to tackle this issue for the case of scalar field theory. Our main result is that the worldsheet picture indeed survives renormalization: all necessary counter-terms have a local worldsheet interpretation for the scalar case. We defer the corresponding study of gauge theories and supersymmetric field theories to future articles.

The lightcone worldsheet [10] is naturally based on light-cone coordinates: an imaginary time  $\tau = ix^+ = i(t + z)/\sqrt{2}$  in the range  $0 \leq \tau \leq T$  and a worldsheet spatial coordinate  $0 \leq \sigma \leq p^+$  chosen so that the  $p^+$  density is uniform. The worldsheet path integral representation of an arbitrary planar diagram is built from the worldsheet path integral for a single scalar propagator [4], which in the massless case, is simply

$$\exp \left\{ -\frac{T\mathbf{p}^2}{2p^+} \right\} = \int DcDbD\mathbf{q} e^{-S} \quad (1)$$

$$S = \int_0^T d\tau \int_0^{p^+} d\sigma \left[ \frac{1}{2}\mathbf{q}^{\prime 2} - \mathbf{b}'\mathbf{c}' \right] \quad (2)$$

where Dirichlet boundary conditions,  $\mathbf{q}(0, \tau) = \mathbf{q}_1$ ,  $\mathbf{q}(p^+, \tau) = \mathbf{q}_2$ , with  $\mathbf{q}_2 - \mathbf{q}_1 = \mathbf{p}$ , are imposed on the bosonic worldsheet variables  $\mathbf{q}(\sigma, \tau)$ . The Grassmann variables  $\mathbf{b}(\sigma, \tau)$ ,  $\mathbf{c}(\sigma, \tau)$  are also subject to Dirichlet conditions:  $\mathbf{b}(0, \tau) = \mathbf{c}(0, \tau) = \mathbf{b}(p^+, \tau) = \mathbf{c}(p^+, \tau) = 0$ . The worldsheet formalism maps every planar diagram to a worldsheet with several internal boundaries each at fixed values of  $\sigma$ . The length and location of each of these internal boundaries are of course integrated over the whole worldsheet. The worldsheet target space fields  $\mathbf{q}(\sigma, \tau)$  satisfy Dirichlet conditions  $\mathbf{q} = \mathbf{q}_i$  on the  $i$ th boundary, and each  $\mathbf{q}_i$  is integrated (the momenta flowing through the propagators of the multi-loop diagram are obtained from the  $\mathbf{q}_i$  as the various differences  $\mathbf{q}_i - \mathbf{q}_j$ ). The ghosts satisfy  $\mathbf{b} = \mathbf{c} = 0$  on each internal boundary.

Since the focus of this article is the renormalization of individual Feynman diagrams, the fine details of the worldsheet construction will not play a central role except to dictate a regularization of the diagrams which enables a rigorous passage from worldsheet picture to conventional Feynman diagram and *vice versa*. For its rigorous definition the worldsheet formalism relies on a discretization of  $\sigma, \tau$ , and hence of  $T_i, p_i^+$  the light cone times and longitudinal momenta associated with the various propagators of the diagram. On the other

hand, conventional Feynman diagrams require continuous  $T_i, p_i^+$ . The ultraviolet divergences of quantum field theory correspond in lightcone variables to infinities due to integration at large transverse momentum. These transverse momentum infinities will get entangled with, and will spoil, the continuum limit of the  $T_i, p_i^+$  unless they are regulated independently of these longitudinal variables [11, 12]. The requirement that this transverse regulator be local on the worldsheet then dictates that it be applied only to the boundary values  $q_i$ . Such a cutoff is local in both  $\sigma, \tau$  because it only need be applied at the beginning or end of an internal boundary (because of the Dirichlet conditions), i.e. at a point on the worldsheet. It is particularly convenient for our analysis to simply impose a Gaussian cutoff, i.e. to insert in the integrand the factor  $e^{-\delta \sum q_i^2}$  [12–14]. This factor can be directly interpreted as a local modification of the worldsheet action.

With  $\delta > 0$  and fixed, the rigorously defined world sheet path integral for each multi-loop planar diagram can be explicitly evaluated on the worldsheet lattice [15] and then the continuum limit of the  $T_i, p_i^+$  for the various propagators can be safely taken. The result, essentially by construction, reduces to one of the standard representations of the Feynman diagram in momentum space with the regulator factor  $e^{-\delta \sum q_i^2}$  inserted in the integrand. Because the  $\delta$  regulator is in place, these integrals are manifestly finite. In Section 2 we describe how this reduction takes place.

After this reduction, there remains an almost conventional analysis of the renormalization procedure in the context of this somewhat novel regulator. The novelty stems from the fact that the  $q_i$ 's, the variables subject to the cut-off, are not the momenta flowing through the propagators. Rather, they are “dual-momentum” variables, one assigned to each loop. There is also a set of external dual-momenta  $q_i^e$ , one assigned to each region between external lines. The momentum flowing through the propagator that separates loop  $i$  from loop  $j$  is the difference  $q_i - q_j$ . Thus the regulator breaks a “translation” symmetry  $q_i^e \rightarrow q_i^e + a$  enjoyed by the *bare* unregulated diagram<sup>3</sup>. Because of this broken symmetry, with  $\delta > 0$  the  $n$ -point function depends on  $n$  dual-momenta rather than on  $n - 1$  actual momenta. Formally the limit  $\delta \rightarrow 0$  should restore the symmetry and the amplitudes should become independent of one of the dual-momenta. Because of ultraviolet divergences, the introduction of counter-terms is necessary to ensure that this happens.

In Section 3 we describe the properties of this regularization in great detail. In section 4 we discuss the self-energy and its renormalization through two loops by direct calculation. Then an all orders argument is constructed in Section 5. The one loop three point vertex is calculated in Section 6, and the correct asymptotically free behavior is confirmed. Finally in the concluding Section 7 we return to the worldsheet formalism and show how the new counter-terms required by renormalization can be represented locally on the worldsheet.

## 2 From the Worldsheet to the Schwinger Representation

In this article we will not need much of the detailed worldsheet formalism, which is rigorously defined on a worldsheet lattice. But for the reader’s convenience we review the worldsheet construction for scalar field theory in an appendix. By construction, the evaluation of the worldsheet path integral representing a specific planar Feynman diagram produces a certain discretized version of the usual multi-loop integral. Each propagator appears in its mixed  $\mathbf{p}, p^+ > 0, x^+$  representation

$$\begin{aligned} \int \frac{dp^-}{2\pi} e^{-ix^+ p^-} \frac{-i}{p^2 + \mu_0^2 - i\epsilon} &= \frac{\theta(x^+)}{2p^+} e^{-ix^+ (\mathbf{p}^2 + \mu_0^2)/2p^+} \\ &\rightarrow \frac{\theta(\tau)}{2p^+} e^{-\tau (\mathbf{p}^2 + \mu_0^2)/2p^+}. \end{aligned} \quad (3)$$

The Feynman integration is over all independent  $\tau_i, p_i^+, \mathbf{p}_i$ . However the worldsheet lattice formalism produces instead sums over discretized  $\tau_i = k_i a, p_i^+ = l_i m$ , while keeping the  $\mathbf{p}_i$  integrals continuous. However, in the presence of the regulator  $\delta > 0$  described in the introduction, one can safely replace all of the discretized sums by continuous integrals.

---

<sup>3</sup>Because the regulator only cuts off the transverse components of  $q$ , the translation symmetry in the longitudinal momenta remains unbroken.

We would like to now show that these perhaps unfamiliar lightcone multi-loop integrals are identical to the covariant Feynman integrals in which each propagator is written in a Schwinger representation.

$$\frac{1}{p^2 + \mu^2} = \int_0^\infty dT e^{-T(p^2 + \mu^2)}. \quad (4)$$

Indeed, it is straightforward to show that the number of independent  $\tau_i, p_i^+$  in the diagram's lightcone representation is precisely equal to the number of  $T_i$  in the diagram's Schwinger representation. If one explicitly carries out the Gaussian integrals in the two representations by completing the square the remaining integrals in the two representations will be of the same dimensionality. The integrands are very similar except that the determinant prefactor from the lightcone is raised to the  $(D-2)/2$  power compared to the  $D/2$  power in the Schwinger representation. One can make the exponentials in the integrands identical by changing integration variables from the  $\tau_i, p_i^+$  to appropriate  $T_i$ . It then turns out that the Jacobian for this change of variables supplies the missing determinant factors.

To understand why this happens, just consider the transform to light-cone representation of the Schwinger representation:

$$\begin{aligned} -i \int \frac{dp^-}{2\pi} e^{-ix^+ p^-} \int idT e^{-iT(\mathbf{p}^2 + \mu_0^2 - 2p^+ p^- - i\epsilon)} &= -i \int idT \delta(x^+ - 2p^+ T) e^{-iT(\mathbf{p}^2 + \mu_0^2)} \\ &\rightarrow \int dT \delta(\tau - 2p^+ T) e^{-T(\mathbf{p}^2 + \mu_0^2)}. \end{aligned} \quad (5)$$

From this result we see that the appropriate change of variables is  $T = \tau/2p^+$ . It is interesting and satisfying that the passage to imaginary  $x^+$  in the lightcone representation is completely equivalent to writing the Schwinger representation with a real exponential, which of course is only meaningful after the Wick rotation to Euclidean space.

For the rest of the discussion of renormalization we need no longer refer to the explicit worldsheet representation. We only have to write the usual covariant rules using dual momenta  $q_i$ , and insert the regulator factor  $e^{-\delta \sum_i q_i^2}$ . Once we have established the form of the counter-terms required for renormalization we shall return to give their worldsheet representation at the end of the article.

### 3 Regularization

Draw an arbitrary planar diagram so that its lines divide the plane into different regions, the external lines all going off to infinity. Then the external lines bound infinite regions, and the finite regions fill each loop of the multi-loop diagram. For each loop introduce a momentum  $q_i^\mu$ , assigned to the loop's region. Then each propagator line separates two regions, say  $i_1$  and  $i_2$ , and the propagator's momentum is then taken to be  $q_{i_1} - q_{i_2}$ , and momentum is automatically conserved. We regulate each diagram by including in the integrand the factor  $e^{-\delta \sum_{i=1}^L q_i^2}$ . Since we are using a light-cone world sheet we only cut off the transverse momentum integrals, because we want to preserve longitudinal boost invariance<sup>4</sup>. This regularization sacrifices full Lorentz invariance, but respects the  $O(D-2)$  rotational invariance in transverse space as well as the longitudinal boost invariance. The transverse boost invariances generated by  $M^{\pm i}$  are broken, and it will require counter-terms to restore them in the renormalizable case of 6 space-time dimensions. The task of the worldsheet renormalization program is to enumerate all of the necessary counter-terms and show that each has a local worldsheet interpretation.

Without loss of generality, we can and do restrict attention to proper (*i.e.* connected one particle irreducible) diagrams, with propagators removed from external legs. Such diagrams never have tadpole sub-diagrams, which would be problematic for the lightcone description (because  $p^+ > 0$ ), though not for a covariant description. The only 1PIR diagram involving a tadpole is the one-point function itself,  $\langle \Phi \rangle$ . It is true that the lightcone description has no convenient representation of the one point function. However,

<sup>4</sup>One could easily extent the cutoff to the longitudinal variables, but then the light-cone interpretation would be obscured.

in a covariant description, the only effect of tadpoles as sub-diagrams in larger (improper) diagrams is pure mass renormalization, which means their effect can be absorbed in an additive constant in the self-energy counter-term. In this article we assume that this is always done and therefore drop tadpoles completely. Then we can freely pass back and forth between light-cone and covariant descriptions, as long as we refrain from considering the one-point function itself. Since the one-point function cannot be directly measured in any case, this is no limitation on the lightcone description. If needed, the value of the one-point function can be related via the field equations to  $\langle \Phi^2 \rangle$ , which in turn can be extracted from the high momentum limit of the two point function.

It is convenient to employ the Schwinger representation of each propagator (4):

$$\frac{1}{p^2 + \mu^2} = \int_0^\infty dT e^{-T(p^2 + \mu^2)}$$

which enables the execution of all loop momentum integrals by completing the square in the exponents of the Gaussian integrals. To describe this for an  $L$  loop diagram, assemble the loop momenta in an  $L$  dimensional vector  $q$  and call  $M_0$  the  $L \times L$  symmetric matrix that describes the quadratic terms in the  $q_i$ , so the exponent reads

$$-q^T \cdot (M_0 + \delta)q + v^T \cdot q + q^T \cdot v - B \quad (6)$$

where the  $L$ -vector  $v$  describes the couplings to the momenta assigned to the external regions and  $B$  is a bilinear form in those external momenta. It is understood that  $\delta \neq 0$  only for the transverse components. Then the result of the loop integrations is just

$$\begin{aligned} & \frac{\pi^L}{\det M_0} \left( \frac{\pi^L}{\det(\delta + M_0)} \right)^{(D-2)/2} \exp \left\{ -B + v^T \cdot \frac{1}{\delta + M_0} v \right\} = \\ & \frac{\pi^L}{\det M_0} \left( \frac{\pi^L}{\det(\delta + M_0)} \right)^{(D-2)/2} \exp \left\{ -B + v^T \cdot \frac{1}{M_0} v - \delta \mathbf{v}^T \frac{1}{M_0} \cdot \frac{1}{\delta + M_0} \mathbf{v} \right\} \end{aligned} \quad (7)$$

We see that the shift of  $M_0$  by  $\delta$  regulates the integration region near the zeroes of the determinant, which is the source of ultraviolet divergences in the diagram. The first two terms in the exponent are manifestly Lorentz invariant and are precisely what they would be in the unregulated theory. The last term in the exponent breaks Lorentz invariance because it depends explicitly on the transverse momentum components. If we could argue that it were negligible (as  $\delta \rightarrow 0$ ), we could assert from the known proofs of renormalizability that all divergences as  $\delta \rightarrow 0$  could be covariantly absorbed in the renormalization of mass  $\mu$  and coupling  $g$  to all orders in perturbation theory.

The term in question is nominally of order  $O(\delta)$  but since it also depends on the  $T_i$ 's we must check this estimate more carefully. First note that  $q_0 \equiv (\delta + M_0)^{-1} \mathbf{v}$  is in fact the location of the minimum of a bilinear form in the  $q_i$ 's that has the interpretation as the potential energy of  $L$  particles tied to each other and to the fixed external momenta with a bunch of springs with spring constants  $T_i > 0$  and to the origin with springs of spring constant  $\delta$ . It is obvious that the resulting equilibrium has every  $q_{0i}$  within the simplex with vertices at the origin and the external momenta. If  $\delta = 0$  they are within the simplex with vertices at the external momenta. In either case it follows that  $|q_{0i}|$  is uniformly bounded by the largest external momentum. Thus we can conclude that the term in question is uniformly bounded over the whole integration region by  $L\delta |q_{ext}|_{max}^2$ . Thus the  $O(\delta)$  estimate is rigorous.

Even so, Lorentz non-covariance can survive due to ultraviolet divergences of degree  $1/\delta$  or worse which can overwhelm the  $O(\delta)$  suppression. Fortunately, in a renormalizable theory we can isolate where these divergences can occur and accordingly identify the subtractions necessary to remove these contributions which would violate Lorentz invariance. Indeed the ultraviolet divergences in vertex parts are only logarithmic in  $\delta$  while those in self-energy parts are  $O(1/\delta)$ . Thus we can focus on the self-energy divergences, but of course we must follow their impact as sub-diagrams in larger diagrams as well. Our strategy will be first to directly analyze one and two loop diagrams and then to develop a recursive argument that the subtraction procedure works to all orders.

Before turning to the renormalization procedure, let us establish rigorous limitations on how non-covariant effects can contribute to a general regulated bare diagram. We can expand the non-covariant factor in powers of  $\delta$

$$\exp\left\{-\delta\mathbf{v}^T\frac{1}{M_0}\cdot\frac{1}{\delta+M_0}\mathbf{v}\right\}=\sum_{n=0}\frac{1}{n!}\left(-\delta\mathbf{v}^T\frac{1}{M_0}\cdot\frac{1}{\delta+M_0}\mathbf{v}\right)^n\quad(8)$$

For a fixed diagram with  $L$  loops, this series will terminate at a finite  $n\leq L$  when  $\delta\rightarrow 0$ , because the worst divergence one will encounter is a  $1/\delta$  for each self-energy insertion and the number of independent self energy insertions is obviously bounded by  $L$ , the number of loops. Thus we can conclude that, at worst, the explicit dependence on the transverse momenta is a polynomial of order  $\leq L$  with (possibly divergent) but Lorentz invariant coefficients. Furthermore, since transverse  $O(D-2)$  rotational invariance is maintained by the regularization the polynomial must be a rotational scalar.

The divergences in skeleton diagrams are primitive, coming entirely from the region of integration where all propagator momenta are large, and given by the superficial divergence of the diagram as all internal momenta get large together. In the renormalizable case ( $D=6$ ), 3-point function skeletons are log divergent and will be covariant as  $\delta\rightarrow 0$ . The only skeleton self-energy diagram is the one loop bubble, which has a  $1/\delta$  divergence, so non-covariance in it as  $\delta\rightarrow 0$  resides in a quadratic polynomial in the  $q$ 's. If, following Ward, we develop a diagrammatic expansion of the derivative of the self energy,  $\partial\Pi(q,q')/\partial q^\mu$ , there will be an infinite number of skeleton contributions. Because  $\Pi$  is symmetric under  $q\leftrightarrow q'$  it is uniquely determined by this derivative up to an additive constant. The skeletons contributing to this derivative of the self energy are linearly divergent and their non-covariant contributions will be simply linear in the transverse momenta. Furthermore, since the divergences in skeletons require all momenta to be large, the coefficients of these polynomials must be constants.

Let us summarize the situation for skeleton diagrams. The derivative of the self energy is linearly divergent: both its infinity and  $\delta$  artifacts are canceled by a counter-term of the form

$$\frac{\partial}{\partial q^\mu}\Pi_{\text{C.T.}}=\frac{\partial}{\partial q^\mu}\left(-\alpha\mathbf{q}^2-\beta(\mathbf{q}-\mathbf{q}')^2+(Z^{-1}-1)(q-q')^2\right)\quad(9)$$

which implies by symmetry

$$\Pi_{\text{C.T.}}=\delta\mu^2-\alpha(\mathbf{q}^2+\mathbf{q}'^2)-\beta(\mathbf{q}-\mathbf{q}')^2+(Z^{-1}-1)\left((q-q')^2+\mu^2\right).\quad(10)$$

The three point skeletons are logarithmically divergent and will possess no  $\delta$  artifacts. The infinity is canceled by a constant counter-term

$$\Gamma_{\text{C.T.}}^3=gZ^{-3/2}(Z_1-1).\quad(11)$$

All higher point skeletons are finite.

On the other hand the infinities and  $\delta$  artifacts caused by divergences in sub-diagrams can be higher order polynomials than the superficial divergence indicates, and the coefficients can depend non-analytically on the Lorentz invariants constructed from the external momenta. Indeed, powers of transverse momenta higher than the superficial divergence must, for dimensional reasons, be multiplied by reciprocal powers of momenta or mass, implying non-analyticity. In a conventional regularization scheme, divergent sub-diagrams are automatically taken care of by the renormalization subtractions performed on primitive diagrams at lower orders of perturbation theory. Since the  $\delta$  regularization is not quite of the conventional type, we need to show that this procedure continues to properly handle sub-diagram artifacts in spite of its novel features.

The necessary counter-terms established by consideration of skeleton diagrams can be incorporated in the theory by choosing the bare propagator

$$\Delta_0(q,q')=\frac{1}{(q-q')^2+\mu_0^2+\alpha(\mathbf{q}^2+\mathbf{q}'^2)+\beta(\mathbf{q}-\mathbf{q}')^2}\quad(12)$$

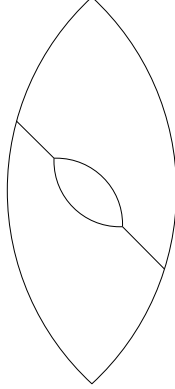


Figure 1: A three loop diagram.

and by renormalizing the bare parameters  $\mu_0, g_0$ . The parameters  $\alpha, \beta$  parameterize violations of Lorentz invariance in the zeroth order theory which are to be tuned to cancel the violations generated by residual artifacts as  $\delta \rightarrow 0$ . To examine how this works in perturbation theory, we might attempt to assume  $\alpha = \beta = 0$  at zero coupling and expand the bare propagator in powers of  $\alpha, \beta$ . However such a naïve approach runs into the difficulty that there are regions of momentum integration where  $\mathbf{q}^2, \mathbf{q}'^2 \gg \mu^2, (q - q')^2$ , and in these regions the  $n$ th term in the expansion of the propagator about  $\alpha = \beta = 0$  blows up like  $\mathbf{q}^{2n}/\mu^{2n}$ , ruining the power counting behind renormalizability. This difficulty first arises in three-loop diagrams such as Fig. 3 which is the lowest order diagram with a self-energy insertion on a line that does not border the planar diagram. Note that this issue does not arise in conventional regularizations because then the propagator, including potential counter terms, depends only on the momentum differences, so powers of momentum in the numerator are always compensated by corresponding powers in the denominator. The same compensation will occur in the  $\delta$  regularization provided that we study renormalization with  $\alpha \rightarrow \epsilon > 0$  at zero coupling. Then the renormalized parameters of the theory are  $\mu, g, \epsilon$  all held fixed as  $\delta \rightarrow 0$ , while  $\mu_0, g_0, \beta, \alpha - \epsilon$  are adjusted so that infinities and  $\delta$  artifacts are canceled order by order in perturbation theory in  $g$ . Only at the very end of the calculation, after renormalization and after the limit  $\delta \rightarrow 0$  do we set  $\epsilon = 0$  and recover full Lorentz invariance<sup>5</sup>. To identify the self energy counter-term we introduce the renormalized mass  $\mu^2 = \mu_0^2 + \delta\mu^2$  and allow for wave function renormalization  $Z$ . Then expanding the bare propagator we find

$$\Delta_0(q, q', \epsilon) = \sum_{n=0}^{\infty} \frac{Z^{n+1}}{[(q - q')^2 + \mu^2 + \epsilon(\mathbf{q}^2 + \mathbf{q}'^2)]^{n+1}} (\text{P.C.T.})^n \quad (13)$$

$$\text{P.C.T.} = \delta\mu^2 + \left(\frac{1}{Z} - 1\right) [(q - q')^2 + \mu^2] - \left(\alpha - \frac{\epsilon}{Z}\right) (\mathbf{q}^2 + \mathbf{q}'^2) - \beta(\mathbf{q} - \mathbf{q}')^2 \quad (14)$$

Keeping  $\epsilon \neq 0$  modifies the analysis of  $\delta$  dependence slightly. The matrix  $M_0$  in (6) is changed, when acting on the transverse variables, to  $M_\epsilon \equiv M_0 + \epsilon M_0^{\text{diag}}$  where  $M^{\text{diag}}$  means the matrix obtained by dropping the off-diagonal elements of the matrix  $M$ . Also the bilinear in external momenta  $B$  acquires a term linear

<sup>5</sup>Organizing the perturbative expansion in this way corresponds to the way a nonperturbative evaluation of the worldsheet path integral would be done. Namely, one would evaluate a physical quantity at finite  $\delta$  and fixed  $\alpha, \beta, g_0, \mu_0$ . Then one would study how the scaling behavior as  $\delta \rightarrow 0$  depends on these bare parameters searching for parameter sets that give Lorentz invariant predictions. Another way to organize the perturbative calculation, which would automatically give the usual Lorentz invariant result, would be to send  $\delta \rightarrow 0$  inside out, starting with the “innermost” integrals together with their counter-terms before doing the next outer loop integration. This would automatically reproduce the standard BPHZ subtraction procedure. We need to deal with the situation where all momentum integrals and subtractions are done at finite  $\delta$ , and  $\delta \rightarrow 0$  afterwards. Different ways of organizing the  $\delta \rightarrow 0$  limit must give the same results in terms of physical renormalized parameters, but they need not, and in general will not, give the same relations of physical parameters to bare parameters.

in  $\epsilon$ ,  $B \rightarrow B_\epsilon = B + \epsilon B_\perp$  where  $B_\perp$  is obtained from  $B$  by dropping the terms in longitudinal momenta. Then the result of doing the momentum integrations (7) now reads:

$$\begin{aligned} & \frac{\pi^L}{\det M_0} \left( \frac{\pi^L}{\det(\delta + M_\epsilon)} \right)^{(D-2)/2} \exp \left\{ -B_\epsilon + v^T \cdot \frac{1}{\delta + M_\epsilon} v \right\} = \\ & \frac{\pi^L}{\det M_0} \left( \frac{\pi^L}{\det(\delta + M_\epsilon)} \right)^{(D-2)/2} \exp \left\{ -B_\epsilon + v^T \cdot \frac{1}{M_\epsilon} v - \delta v^T \frac{1}{M_\epsilon} \cdot \frac{1}{\delta + M_\epsilon} v \right\} \end{aligned} \quad (15)$$

where it is understood that  $M_\epsilon$  is replaced by  $M_0$  for the longitudinal components. The argument that the  $\delta$  dependent term in the exponent is uniformly of order  $O(\delta)$  over the whole integration region remains valid. Thus as  $\delta \rightarrow 0$  that term only gives contributions when multiplying divergences of order  $1/\delta$  or worse which can only come from self energy insertions. Of course with  $\epsilon \neq 0$ , removing these contributions by suitable counter-terms will not restore Lorentz covariance. But all of the residual non-covariance will disappear when we set  $\epsilon = 0$  at the end of the calculation.

## 4 Self Energy for $\Phi^3$

In order to acquaint the reader with some of the novelties of calculations using the  $\delta$  regulator, we carry out in this section a direct calculation of the self energy through two loops, with an explicit separation of all divergences and Lorentz-violating artifacts. Since keeping  $\epsilon > 0$  is not essential through two loop order, we shall for simplicity set  $\epsilon = 0$  for most of the calculation. However, as an example to show that  $\epsilon \neq 0$  causes no special difficulties, we shall show the one loop calculation with  $\epsilon > 0$ . We call the bare self-energy  $\Pi_0$ , but it is convenient to calculate  $Z\Pi_0$  and absorb the factor of  $Z$  in the bare coupling by defining the renormalized coupling  $g = g_0 Z^{3/2}/Z_1$ , where  $Z_1$  is the three vertex renormalization constant. In other words we write down the Feynman rules in terms of renormalized mass and coupling, canceling infinities against the self-energy counter-term  $Z\Pi_{C.T.}$  (see (14) and the three vertex counter-term  $g(Z_1 - 1)\Phi^3$ , which are included in the Feynman rules, rather than absorbing them in redefinitions of the bare parameters.

### 4.1 One Loop

The unsubtracted one-loop self-energy diagram has the value

$$\begin{aligned} Z\Pi_0 &= \frac{g^2}{(4\pi)^3} \int_0^\infty \frac{dT_1 dT_2}{(T_1 + T_2)(T_1 + T_2 + \delta)^2} \\ & \quad \exp \left\{ -\mu^2(T_1 + T_2) - \frac{T_1 T_2}{T_1 + T_2} (q - q')^2 - \delta \frac{(T_1 \mathbf{q} + T_2 \mathbf{q}')^2}{(T_1 + T_2)(T_1 + T_2 + \delta)} \right\} \\ Z\Pi_0 &= \frac{g^2}{(4\pi)^3} \int_0^\infty \frac{dT e^{-\mu^2 T}}{(T + \delta)^2} \int_0^1 dx \exp \left\{ -Tx(1-x)(q - q')^2 - \frac{\delta T}{T + \delta} (x\mathbf{q} + (1-x)\mathbf{q}')^2 \right\} \end{aligned} \quad (16)$$

The quadratic divergence can be simply extracted with an integration by parts, and the log divergence isolated by one further subtraction in the remaining integrand

$$\begin{aligned} Z\Pi_0 &= -\frac{g^2}{(4\pi)^3} \int_0^\infty \frac{dT}{T + \delta} \int_0^1 dx \left[ H_0 (e^{-HT} - e^{-\mu^2 T}) + \frac{\delta^2 (x\mathbf{q} + (1-x)\mathbf{q}')^2}{(T + \delta)^2} (e^{-HT} - 1) \right] \\ & \quad + \frac{g^2}{(4\pi)^3} \left\{ \frac{1}{\delta} - \int_0^1 dx \left[ H_0 I(\mu^2 \delta) + \frac{1}{2} (x\mathbf{q} + (1-x)\mathbf{q}')^2 \right] \right\} \end{aligned} \quad (17)$$

$$H \equiv \mu^2 + x(1-x)(q - q')^2 + \frac{\delta}{T + \delta} (x\mathbf{q} + (1-x)\mathbf{q}')^2 \equiv H_0 + \frac{\delta}{T + \delta} (x\mathbf{q} + (1-x)\mathbf{q}')^2 \quad (18)$$

$$I(t) \equiv \int_0^\infty \frac{e^{-ut} du}{1+u} \underset{t \rightarrow 0}{\sim} \ln \frac{1}{t} \quad (19)$$



We can choose the first order contribution of the self energy counter term (14),  $Z\Pi_{\text{C.T.}}^{(1)}$ , to cancel the second line, which will then cancel the divergences as well as the Lorentz violating term which would survive the  $\delta \rightarrow 0$  limit. In particular we find for the wave function renormalization to this order,

$$Z^{(1)} = 1 - \frac{1}{6} \frac{g^2}{(4\pi)^3} I(\mu^2\delta) \quad (20)$$

Thus we write the one-loop renormalized self energy (at finite  $\delta$ ) as

$$\begin{aligned} \Pi^{(1)} &\equiv Z(\Pi_0 + \Pi_{\text{C.T.}}^{(1)}) \\ &= -\frac{g^2}{(4\pi)^3} \int_0^\infty \frac{dT}{T+\delta} \int_0^1 dx \left[ H_0(e^{-HT} - e^{-\mu^2 T}) + \frac{\delta^2(x\mathbf{q} + (1-x)\mathbf{q}')^2}{(T+\delta)^2} (e^{-HT} - 1) \right] \end{aligned} \quad (21)$$

As long as  $\delta > 0$  Lorentz invariance is clearly violated by the explicit dependence of this expression on the transverse components of the momenta. However, because of the subtracted counter-term these violations disappear in the limit  $\delta \rightarrow 0$  at fixed  $q, q'$ . Indeed, in this limit the second term in square brackets  $O(\delta)$  and the expression  $HT$  in the first term tends to  $H_0T + O(\delta \ln \delta)$ , so we have

$$\Pi_1 \sim -\frac{g^2}{(4\pi)^3} \int_0^\infty \frac{dT}{T} \int_0^1 dx H_0(e^{-H_0T} - e^{-\mu^2 T}) = \frac{g^2}{(4\pi)^3} \int_0^1 dx H_0 \ln \frac{H_0}{\mu^2} \quad (22)$$

which is obviously Lorentz invariant and finite.

Before moving on to two loops, we pause to indicate how  $\epsilon \neq 0$  complicates the one loop calculation. Then we use the more general free propagator

$$\frac{Z}{\mu^2 + (q - q')^2 + \epsilon(\mathbf{q}^2 + \mathbf{q}'^2)}, \quad (23)$$

associated with the self energy counter-term (14). Now the bare unsubtracted one-loop self energy is

$$\begin{aligned} Z\Pi_0 &= \frac{g^2}{(4\pi)^3} \int_0^\infty \frac{dT_1 dT_2}{(T_1 + T_2)[(T_1 + T_2)(1 + \epsilon) + \delta]^2} \exp \left\{ -\delta \frac{(T_1\mathbf{q} + T_2\mathbf{q}')^2}{(1 + \epsilon)(T_1 + T_2)[(T_1 + T_2)(1 + \epsilon) + \delta]} \right\} \\ &\quad \exp \left\{ -\mu^2(T_1 + T_2) - \frac{T_1 T_2}{T_1 + T_2} (q - q')^2 - \epsilon[T_1\mathbf{q}^2 + T_2\mathbf{q}'^2] - \frac{\epsilon}{1 + \epsilon} \frac{(T_1\mathbf{q} + T_2\mathbf{q}')^2}{T_1 + T_2} \right\} \\ Z\Pi_0 &= \frac{g^2}{(4\pi)^3} \int_0^\infty \frac{dT}{(T(1 + \epsilon) + \delta)^2} \int_0^1 dx \exp \left\{ -TH_\epsilon - \frac{\delta T}{(1 + \epsilon)(T(1 + \epsilon) + \delta)} (x\mathbf{q} + (1-x)\mathbf{q}')^2 \right\} \end{aligned} \quad (24)$$

$$H_\epsilon = \mu^2 + x(1-x)(q - q')^2 + \epsilon[x\mathbf{q}^2 + (1-x)\mathbf{q}'^2] + \frac{\epsilon}{1 + \epsilon} (x\mathbf{q} + (1-x)\mathbf{q}')^2 \quad (25)$$

As before, integration by parts and a subtraction in the remaining integrand isolates the divergences:

$$\begin{aligned} Z\Pi_0 &= \\ &= -\frac{g^2}{(4\pi)^3} \int_0^\infty \frac{dT}{(1 + \epsilon)(T(1 + \epsilon) + \delta)} \int_0^1 dx \left[ H_\epsilon(e^{-HT} - e^{-\mu^2 T}) + \frac{\delta^2(x\mathbf{q} + (1-x)\mathbf{q}')^2}{(1 + \epsilon)(T(1 + \epsilon) + \delta)^2} (e^{-HT} - 1) \right] \\ &\quad + \frac{g^2}{(4\pi)^3} \left\{ \frac{1}{(1 + \epsilon)\delta} - \int_0^1 dx \left[ H_\epsilon \frac{I(\mu^2\delta/(1 + \epsilon))}{(1 + \epsilon)^2} + \frac{1}{2(1 + \epsilon)^3} (x\mathbf{q} + (1-x)\mathbf{q}')^2 \right] \right\} \end{aligned} \quad (26)$$

$$H \equiv H_\epsilon + \frac{\delta(x\mathbf{q} + (1-x)\mathbf{q}')^2}{(1 + \epsilon)(T(1 + \epsilon) + \delta)} \quad (27)$$

We choose  $\Pi_{\text{C.T.}}^{(1)}$  to cancel the third line obtaining for the renormalized self energy for  $\delta, \epsilon > 0$

$$\begin{aligned} \Pi_1 &= \\ &= -\frac{g^2}{(4\pi)^3} \int_0^\infty \frac{dT}{(1 + \epsilon)(T(1 + \epsilon) + \delta)} \int_0^1 dx \left[ H_\epsilon(e^{-HT} - e^{-\mu^2 T}) + \frac{\delta^2(x\mathbf{q} + (1-x)\mathbf{q}')^2}{(1 + \epsilon)(T(1 + \epsilon) + \delta)^2} (e^{-HT} - 1) \right] \end{aligned} \quad (28)$$

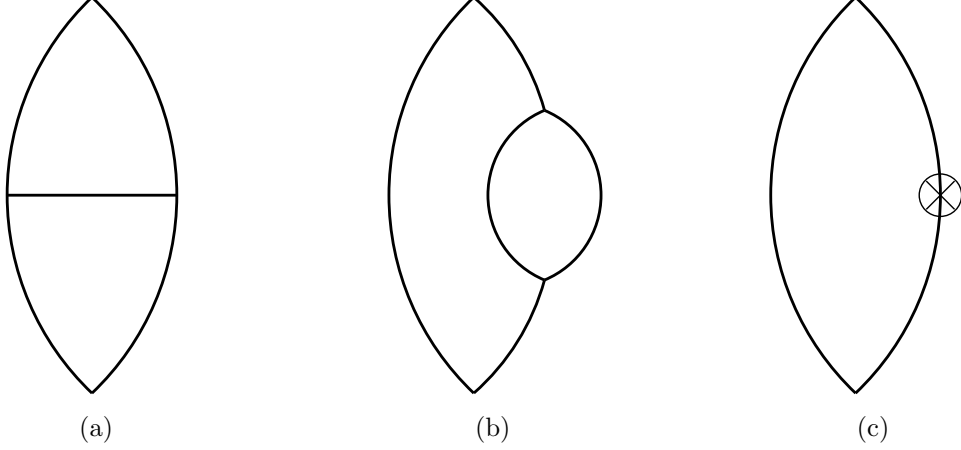


Figure 2: Self energy two loop diagrams

and (20) changes to

$$Z_\epsilon^{(1)} = 1 - \frac{1}{6} \frac{g^2}{(4\pi)^3} \frac{1}{(1+\epsilon)^2} I \left( \frac{\mu^2 \delta}{1+\epsilon} \right) \quad (29)$$

Taking the limit  $\delta \rightarrow 0$  yields

$$\Pi_1 \sim -\frac{g^2}{(4\pi)^3} \int_0^\infty \frac{dT}{(1+\epsilon)^2 T} \int_0^1 dx H_\epsilon (e^{-H_\epsilon T} - e^{-\mu^2 T}) = \frac{1}{(1+\epsilon)^2} \frac{g^2}{(4\pi)^3} \int_0^1 dx H_\epsilon \ln \frac{H_\epsilon}{\mu^2} \quad (30)$$

a finite result, but of course it is not Lorentz invariant unless  $\epsilon = 0$ . Note that there is no particular sensitivity to  $\epsilon$  in this limit. The presence of  $\epsilon \neq 0$  does not change the qualitative power-counting: the self energy grows quadratically with momenta and the propagator falls off quadratically, any number of self energy insertions in a skeleton diagram does not alter the high momentum behavior of the integrand mod logs. The advantage of keeping  $\epsilon > 0$  is that this power counting also holds for  $\delta \neq 0$ .

## 4.2 Two Loops

Now we turn to the two loop self-energy, setting  $\epsilon = 0$  for simplicity. First consider the two loop diagram in Fig.2a). The matrix  $M_0$  and related quantities for this graph are given by

$$M_0 = \begin{pmatrix} T_1 + T_3 + T_5 & -T_5 \\ -T_5 & T_2 + T_4 + T_5 \end{pmatrix} \quad (31)$$

$$\frac{1}{\delta + M_0} = \frac{1}{\det(M_0 + \delta)} \begin{pmatrix} \delta + T_2 + T_4 + T_5 & T_5 \\ T_5 & \delta + T_1 + T_3 + T_5 \end{pmatrix} \quad (32)$$

$$\det(M_0 + \delta) = (\delta + T_1 + T_3 + T_5)(\delta + T_2 + T_4 + T_5) - T_5^2 \quad (33)$$

The vector describing the external momenta is given by

$$v = \begin{pmatrix} T_1 q + T_3 q' \\ T_2 q + T_4 q' \end{pmatrix} \quad (34)$$

so we find

$$\frac{1}{\delta + M_0} v = \frac{1}{\det(M_0 + \delta)} \begin{pmatrix} q(T_1 \delta + T_1(T_2 + T_4 + T_5) + T_2 T_5) + q'(T_3 \delta + T_3(T_2 + T_4 + T_5) + T_4 T_5) \\ q(T_2 \delta + T_2(T_1 + T_3 + T_5) + T_1 T_5) + q'(T_4 \delta + T_4(T_1 + T_3 + T_5) + T_3 T_5) \end{pmatrix} \quad (35)$$

This two loop amplitude in Schwinger representation is

$$\Pi_{2,a}^0 = \frac{g^4}{(4\pi)^6} \int_0^\infty \prod_{i=1}^5 dT_i \frac{1}{\det M_0} \frac{1}{\det(M_0 + \delta)^2} \exp \left\{ -\mu^2 \sum_{i=1}^5 T_i - (q - q')^2 \frac{N(T_i)}{\det M_0} - \delta \mathbf{v}^T \cdot \frac{1}{M_0} \frac{1}{\delta + M_0} \mathbf{v} \right\} \quad (36)$$

$$N(T_i) = T_1 T_2 (T_3 + T_4) + T_3 T_4 (T_1 + T_2) + T_5 (T_1 + T_2) (T_3 + T_4) \quad (37)$$

To analyze the  $\delta \rightarrow 0$  limit we can expand to first order in the last term of the exponent since it is  $O(\delta)$  and the worst divergence in the integration is  $O(1/\delta)$ . Moreover, for this diagram that divergence comes only when all the  $T_i$  are  $O(\delta)$ . Thus the second term of this expansion can be simplified by setting the exponent to zero and scaling all the  $T_i \rightarrow \delta T_i$ , exploiting the homogeneity in the  $T_i$  of the integrand:

$$\text{Second Term} \rightarrow -\frac{g^4}{(4\pi)^6} \int_0^\infty \prod_{i=1}^5 dT_i \frac{1}{\det M_0} \frac{1}{\det(M_0 + 1)^2} \mathbf{v}^T \cdot \frac{1}{M_0} \frac{1}{1 + M_0} \mathbf{v} \quad (38)$$

which is clearly a quadratic polynomial in the transverse components of the external momenta with constant and finite coefficients, which is of the form of the allowed counter-terms for the self-energy. The first term in the expansion is a manifestly covariant regularization of the standard two loop amplitude. It contains the usual logarithmic overlapping divergences that renormalize the vertices of the one loop self energy as well as the overall quadratic  $1/\delta$  divergence that is to be absorbed in the mass, as well as and overall log divergence that contributes to the two loop wave function renormalization. The overall quadratic divergence is easy to extract by dropping the exponent and scaling the  $T_i$ :

$$\text{Quad Divergence} = \frac{1}{\delta} \frac{g^4}{(4\pi)^6} \int_0^\infty \prod_{i=1}^5 dT_i \frac{1}{\det M_0} \frac{1}{\det(M_0 + 1)^2}. \quad (39)$$

The overlapping log divergences correspond either to  $T_1, T_3, T_5 \sim 0$ ,  $T_2, T_4$  finite or  $T_2, T_4, T_5 \sim 0$  with  $T_1, T_3$  finite. For definiteness take the first case. We note the simplifications

$$\begin{aligned} N(T_i) &\rightarrow (T_1 + T_3 + T_5) T_2 T_4 \\ \det(M_0 + \delta) &\rightarrow (\delta + T_1 + T_3 + T_5) (T_2 + T_4 + \delta) \end{aligned}$$

So the integration over small  $T_1, T_3, T_5$  involves

$$\int_{T_1+T_3+T_5 < \Delta} dT_1 dT_3 dT_5 \frac{1}{(T_1 + T_3 + T_5)(\delta + T_1 + T_3 + T_5)^2} = \frac{1}{2} \int_0^\Delta dT \frac{T}{(T + \delta)^2} \sim \frac{1}{2} \ln \frac{\Delta}{\delta} \quad (40)$$

and the corresponding contribution to the self energy is

$$\text{Overlap135} = \frac{g^4}{(4\pi)^6} \frac{1}{2} \ln \frac{\Delta}{\delta} \int_\epsilon^\infty dT_2 dT_4 \frac{e^{-\mu^2(T_2+T_4)}}{(T_2 + T_4)(T_2 + T_4 + \delta)^2} \exp \left\{ -(q - q')^2 \frac{T_2 T_4}{T_2 + T_4} \right\}. \quad (41)$$

This is precisely the vertex renormalization needed to renormalize the charge at one vertex of the one loop self energy. The 245 overlap takes care of the renormalization at the other vertex.

We next take up the two loop diagram shown in Fig.2b). We list the corresponding ingredients of the answer:

$$M_0 = \begin{pmatrix} T_1 + T_2 + T_3 + T_4 & -T_4 \\ -T_4 & T_4 + T_5 \end{pmatrix} \quad (42)$$

$$\frac{1}{\delta + M_0} = \frac{1}{\det(M_0 + \delta)} \begin{pmatrix} \delta + T_4 + T_5 & T_4 \\ T_4 & \delta + T_1 + T_2 + T_3 + T_4 \end{pmatrix} \quad (43)$$

$$\det(M_0 + \delta) = (\delta + T_1 + T_2 + T_3 + T_4)(\delta + T_4 + T_5) - T_4^2 \quad (44)$$

The vector describing the external momenta is

$$v = \begin{pmatrix} T_1 q + (T_2 + T_3) q' \\ T_5 q' \end{pmatrix} \quad (45)$$

so we find

$$\frac{1}{\delta + M_0} v = \frac{1}{\det(M_0 + \delta)} \begin{pmatrix} q T_1 (\delta + T_4 + T_5) + q' [(T_2 + T_3) (\delta + T_4 + T_5) + T_4 T_5] \\ q T_1 T_4 + q' [T_5 (\delta + T_1 + T_2 + T_3 + T_4) + T_4 (T_2 + T_3)] \end{pmatrix} \quad (46)$$

This two loop amplitude in Schwinger representation is

$$\Pi_{2,b}^0 = \frac{g^4}{(4\pi)^6} \int_0^\infty \prod_{i=1}^5 dT_i \frac{1}{\det M_0} \frac{1}{\det(M_0 + \delta)^2} \exp \left\{ -\mu^2 \sum_{i=1}^5 T_i - (q - q')^2 \frac{N(T_i)}{\det M_0} - \delta \mathbf{v}^T \cdot \frac{1}{M_0} \frac{1}{\delta + M_0} \mathbf{v} \right\} \quad (47)$$

$$N(T_i) = T_1 T_4 T_5 + T_1 (T_2 + T_3) (T_4 + T_5) \quad (48)$$

Again it is sufficient expand to first order in the last term of the exponent since it is  $O(\delta)$  and the worst divergence in the integration is  $O(1/\delta)$ . However, for this diagram there is, in addition to an overall  $1/\delta$  divergence coming from the region when all the  $T_i$  are  $O(\delta)$ , a  $1/\delta$  divergence from the region  $T_4, T_5 = O(\delta)$ . As before we can scale all the  $T_i$  by  $\delta$ , obtaining:

Second Term  $\rightarrow$

$$-\frac{g^4}{(4\pi)^6} \int_0^\infty \prod_{i=1}^5 dT_i \frac{1}{\det M_0} \frac{1}{\det(M_0 + 1)^2} \mathbf{v}^T \cdot \frac{1}{M_0} \frac{1}{1 + M_0} \mathbf{v} \exp \left\{ -\mu^2 \delta \sum_{i=1}^5 T_i - \delta (q - q')^2 \frac{N(T_i)}{\det M_0} \right\} \quad (49)$$

In these variables, the exponent must be retained to converge the integral in the region  $T_1, T_2, T_3 \gg T_4, T_5$ . In this region, without the exponent the  $T_4, T_5$  integration is linearly convergent but the  $T_1, T_2, T_3$  integration is log divergent at infinity. Because  $T_4, T_5$  integration converges in any case we can simplify the exponent by neglecting  $T_4, T_5$  compared to  $T_1, T_2, T_3$ .

$$\text{Exponent} \rightarrow -\mu^2 \delta (T_1 + T_2 + T_3) - \delta (q - q')^2 \frac{T_1 (T_2 + T_3)}{T_1 + T_2 + T_3} \quad (50)$$

The prefactors to the exponential in this limit have the behavior

$$\frac{1}{\det M_0} \frac{1}{\det(M_0 + 1)^2} \mathbf{v}^T \cdot \frac{1}{M_0} \frac{1}{1 + M_0} \mathbf{v} \sim \frac{1}{T_{13} T_{45} (T_{13} + 1)^2 (T_{45} + 1)^2} \left[ \frac{(T_1 \mathbf{q} + T_{23} \mathbf{q}')^2}{T_{13} (T_{13} + 1)} + \frac{T_{45}}{T_{45} + 1} (x \mathbf{q}_1 + (1 - x) \mathbf{q}')^2 \right] \quad (51)$$

The shorthand notation used here is  $T_{rs} \equiv \sum_{i=r}^s T_i$ . Also  $x = T_4/T_{45}$ , and  $\mathbf{q}_1$  is the  $\delta \rightarrow 1$  limit of

$$\mathbf{q}_\delta = \frac{T_1 \mathbf{q} + T_{23} \mathbf{q}'}{T_{13} + \delta}$$

In this region the integration over  $T = T_{45}$  at fixed  $x$  can be easily performed. We change variables  $dT_4 dT_5 = dx T dT$ , and find

$$\int dT_4 dT_5 \frac{1}{\det M_0} \frac{1}{\det(M_0 + 1)^2} \mathbf{v}^T \cdot \frac{1}{M_0} \frac{1}{1 + M_0} \mathbf{v} \sim \frac{1}{T_{13} (T_{13} + 1)^2} \left[ \frac{(T_1 \mathbf{q} + T_{23} \mathbf{q}')^2}{T_{13} (T_{13} + 1)} + \frac{1}{2} \int_0^1 dx (x \mathbf{q}_1 + (1 - x) \mathbf{q}')^2 \right] \quad (52)$$

The log divergence at large  $T_1, T_2, T_3$  also will bring dependence on the invariant  $(q - q')^2$  into the coefficients of the Lorentz violating polynomial in the transverse momenta. Thus the diagram of Fig.2b) by

itself cannot be made covariant by our allowed subtractions. However, the self energy insertion is accompanied with a counter-term, corresponding to the diagram in Fig.2c). We shall show that the sum of the two diagrams Fig.2b+c) *can* be made Lorentz invariant.

The cross in the counter-term diagram represents the counter-term insertion required for Lorentz invariance of the one loop self energy:

$$\text{Insertion} = -\frac{g^2}{(4\pi)^3} \left[ \frac{1}{\delta} - \frac{1}{2} \int_0^1 dx (x\mathbf{q}_1 + (1-x)\mathbf{q}')^2 \right] \quad (53)$$

Here  $q_1$  is the loop momentum. Evaluating the counter-term diagram gives

$$\begin{aligned} \Pi_{2\text{C.T.}} &= -\frac{g^4}{(4\pi)^6} \int_0^\infty \frac{dT_1 dT_2 dT_3}{T_{13}(T_{13} + \delta)^2} \left[ \frac{1}{\delta} - \frac{1}{4(T_{13} + \delta)} - \frac{1}{2} \int_0^1 dx (x\mathbf{q}_\delta + (1-x)\mathbf{q}')^2 \right] \\ &\exp \left\{ -\mu^2 T_{13} - (q - q')^2 \frac{T_1(T_{23})}{T_{13}} - \frac{\delta(T_1\mathbf{q} + (T_{23})\mathbf{q}')^2}{T_{13}(T_{13} + \delta)} \right\} \end{aligned} \quad (54)$$

Again we can expand to first order in the last term of the exponent and the second term in the expansion only survives multiplying the first two terms in square brackets. Collecting all the terms quadratic in transverse momenta and scaling out  $\delta$ :

$$\begin{aligned} \Pi_{2\text{C.T.}}^{\text{Quad}} &= -\frac{g^4}{(4\pi)^6} \int_0^\infty \frac{dT_1 dT_2 dT_3}{T_{13}(T_{13} + 1)^2} \exp \left\{ -\mu^2 \delta T_{13} - (q - q')^2 \delta \frac{T_1 T_{23}}{T_{13}} \right\} \\ &\left[ -\left( 1 - \frac{1}{4(T_{13} + 1)} \right) \frac{(T_1\mathbf{q} + T_{23}\mathbf{q}')^2}{T_{13}(T_{13} + 1)} - \frac{1}{2} \int_0^1 dx (x\mathbf{q}_1 + (1-x)\mathbf{q}')^2 \right] \end{aligned} \quad (55)$$

Just as before the exponent must be retained to converge the integration at large  $T_1, T_2, T_3$ . However the term coming from the  $-1/4/(T_{13} + 1)$  in the parentheses within the square brackets is convergent without the exponent. By inspection, we can see that all the other terms will exactly cancel the large  $T_1, T_2, T_3$  behavior of the integrand of (49), providing the extra convergence needed to make the exponent negligible. In summary the non-covariant contribution to the sum of the diagrams of Fig.2bc) has been shown to be

$$\begin{aligned} \Pi_{2bc}^{\text{noncov}} &\rightarrow -\frac{g^4}{(4\pi)^6} \int_0^\infty \frac{dT_1 dT_2 dT_3}{4T_{13}^2 (T_{13} + 1)^4} (T_1\mathbf{q} + T_{23}\mathbf{q}')^2 \\ &- \frac{g^4}{(4\pi)^6} \int_0^\infty \prod_{i=1}^5 dT_i \left[ \frac{1}{\det M_0} \frac{1}{\det(M_0 + 1)^2} \mathbf{v}^T \cdot \frac{1}{M_0} \frac{1}{1 + M_0} \mathbf{v} \right. \\ &\left. - \frac{1}{T_{13} T_{45} (T_{13} + 1)^2 (T_{45} + 1)^2} \left[ \frac{(T_1\mathbf{q} + T_{23}\mathbf{q}')^2}{T_{13}(T_{13} + 1)} + \frac{T_{45}}{T_{45} + 1} (x\mathbf{q}_1 + (1-x)\mathbf{q}')^2 \right] \right] \end{aligned} \quad (56)$$

which, though complicated, is easily seen to be a quadratic polynomial in the transverse momenta with constant coefficients.

## 5 An all orders argument

### 5.1 Preliminaries

In preparation for an all orders argument let us reconsider the two loop self-energy diagrams with an eye to understanding, without detailed calculation, why subtraction of a second order polynomial in momenta suffices to remove the regularization artifacts. For any multi-loop diagram containing no divergent sub-diagrams, the reason is transparent. Then the regularization dependence could only come from the region of loop momentum integration in which *all* internal momenta are large. For this region one can expand in powers of the external momenta, and by power counting all powers of external momenta higher than

quadratic will be negligible. Unfortunately the only self energy diagram with no divergent sub-diagrams is the one loop one. But then we can apply Ward's trick, and calculate the derivative of the self energy instead.

The core of the problem then is to understand how to take care of divergent sub-diagrams. At two loops the only dangerous diagram is the one which has  $\Pi_1$  inserted on one of the propagator lines. We can write the bare regulated two-loop diagram plus the one loop diagram with the counter-term corresponding to the self-energy insertion as

$$\Pi_2^0 = g^2 \int \frac{d^6 q_1}{(2\pi)^6} e^{-\delta q_1^2} \frac{1}{(q_1 - q)^2 + \mu^2} \frac{1}{((q_1 - q')^2 + \mu^2)^2} \Pi_1(q_1, q', \delta). \quad (57)$$

We must now argue that when  $\delta \rightarrow 0$  the Lorentz violations in  $\Pi_2^0$  reside exclusively in a quadratic polynomial in the  $\mathbf{q}, \mathbf{q}'$  with constant coefficients. We first note that the subtractions inherent in the definition of the insertion  $\Pi_1$  guarantee that the Lorentz violations due to  $\Pi_1$  will disappear for any finite region of the  $q_1$  integration. They are only present for  $q_1 > O(1/\delta)$ . But for large  $q_1$ , we can expand the integrand, including  $\Pi_1$  in the external momenta, and integrating over the region  $q_1 > 1/\delta$  will yield a polynomial in all components of the external momenta with coefficients possibly singular in  $\delta$  plus a finite remainder that is Lorentz invariant. The order of this polynomial is limited by power counting to the degree of divergence of the self energy namely 2. Since the regulator preserves both transverse rotational invariance and longitudinal Lorentz invariance, the polynomial must be a linear combination of  $(q - q')^2$ ,  $\mathbf{q}^2$ ,  $\mathbf{q}'^2$ , and  $(\mathbf{q} - \mathbf{q}')^2$ . But this is what was to be proved. Thus one can subtract a suitable counter-term from  $\Pi_2^0$  to obtain  $\Pi_2$  as a covariant function of  $(q - q')^2$  only. This form of the argument can be used to prove by induction that subtraction of a counter-term of the form  $\alpha(g)(\mathbf{q}^2 + \mathbf{q}'^2) + \beta(g)(\mathbf{q} - \mathbf{q}')^2$  from  $\Pi^0$  will be sufficient to render the self energy, as well as all proper diagrams Lorentz invariant to all orders in perturbation theory.

As we carry on beyond two loops, inserting renormalized self energy and vertex diagrams as sub-diagrams in larger diagrams is supposed to take care of the divergences due to sub-integrations. To evaluate the effect of such insertions on the divergence structure of the larger diagram, however, we need to know the large momentum behavior of the renormalized insertions. The usual rule of thumb is that the renormalized propagators and vertex functions have the same high momentum behavior as their free counterparts *modulo* logarithms. In a standard covariant calculational scheme, the self-energy and propagator each depend on the single invariant  $(q - q')^2$ , so this rule of thumb translates to self energies behaving asymptotically like  $(q - q')^2$  and propagators like  $(q - q')^{-2}$ . This has the consequence that the insertion of a self-energy on a line does not alter the asymptotic behavior (mod logs), because each such insertion comes with one extra propagator so there is a cancellation. As discussed in the previous section, in order for this same power counting to be maintained with  $\delta > 0$ , it is important to hold  $\epsilon > 0$  throughout the renormalization procedure. Then positive powers of momentum in the asymptotics of the self energy will be compensated by corresponding negative powers from extra propagators, regardless of which components of the momenta are large. The zeroth order propagator is then  $[(q - q')^2 + \mu^2 + \epsilon(\mathbf{q}^2 + \mathbf{q}'^2)]^{-1}$ , and the extra terms give the inverse free propagator the same generic asymptotic behavior as the self energy.

The original sum of bare diagrams possessed a symmetry under the shift of all the  $q$  momenta by the same constant:  $q_i \rightarrow q_i + a$ . The  $\delta$  regulator destroys this symmetry, and the mismatch in asymptotic behavior between the self energy and the free propagator when  $\epsilon = 0$  and  $\delta > 0$  can be traced to the fact that the free propagator possesses this symmetry while the interactions do not. With  $\epsilon > 0$  the free propagator no longer possesses this symmetry and the power counting rules are restored. Our procedure then is to start with  $\delta$  and  $\epsilon$  non-zero, for which the free propagator violates both the shift symmetry and Lorentz symmetry. We then calculate to some finite order in perturbation theory. Then, after renormalization and adjustment of counter-terms, we take  $\delta \rightarrow 0$  to obtain a finite result containing no  $\delta$  artifacts. The final step is to set  $\epsilon \rightarrow 0$  to restore shift and Lorentz invariance and establish agreement with standard renormalized perturbation theory.

## 5.2 The argument

It is convenient, for purposes of formulating the all orders argument, to dispense with the Schwinger representation and to use the expressions for the multi-loop diagrams as integrals over the  $q$ 's only. We use

induction on  $n$ , the number of loops. Specifically, the induction hypothesis is that through  $n$  loops, the renormalization of  $\mu^2, g$  and adjustment of  $\alpha, \beta$  has rendered all planar 1PIR amplitudes finite when all external momenta are much less than  $1/\delta$  in such a way that the dependence on these external momenta is finite and Lorentz invariant when  $\epsilon = 0$ .

Now consider the  $n + 1$  loop planar diagrams, including all of the counter-terms necessary through  $n$  loop order. Our task is to argue that all new infinities and artifacts that appear in this order can be absorbed in the new counter-terms allowed in this order. Consider first the region of  $q$  integration in which any of the propagators bordering the planar diagram carries momentum much less than the cutoff  $1/\sqrt{\delta}$ . For this region of integration the induction hypothesis is operative, guaranteeing that no infinities or artifacts are present in this region.

Thus we can turn our attention to the region of  $q$  integration where *all* of the propagators bordering the planar diagram carry momenta on the order  $O(1/\sqrt{\delta})$ . In this region it is safe to expand these propagators in powers of the external momenta they depend on. Because the diagram is planar, the external momenta appear nowhere else in the integrand. The coefficient of the  $k$ th power of external momenta in this expansion is in order of magnitude a factor  $(\sqrt{\delta})^k$  times the value of the diagram at 0 external momenta. Since there are a finite number of loops in the diagram of interest, there is a limit on the number of inverse powers of  $\delta$  in this coefficient, so this series must terminate and we conclude that this dangerous region of integration produces at worst a polynomial in all of the external momenta. Simple power counting indicates that this integration region of the self-energy diagrams supply at most a single power of  $1/\delta$ , of the three point functions at most a  $\ln \delta$ , and of the four and higher point functions only positive powers of  $\delta$ . This conclusion does not hold for the unrenormalized diagrams because of the possibility of divergent sub-diagrams. However, including the counter-terms and renormalization through  $n$  loops (which is part of the induction hypothesis) renders these sub-integrations finite and restores the simple power counting. It is crucial however that  $\epsilon$  is held fixed at a positive value during this renormalization process.

The upshot is that at  $n + 1$  loop order the new infinities and artifacts reside in a quadratic polynomial for the self energy, in a constant for the three point function and are absent in the four and higher point functions. But these are exactly of the form of the allowed new counter-terms and the argument is complete.

## 6 The triangle graph and one-loop coupling renormalization

As a final exercise we complete renormalization at one loop by evaluating the 1PIR one loop correction to the cubic vertex in the presence of  $\epsilon > 0$ . We obtain for the one-loop triangle diagram at fixed  $\delta, \epsilon$

$$\begin{aligned}
Z^{3/2}\Gamma_3^{(1)} &= \frac{g^3}{(4\pi)^3} \int_0^\infty \frac{dT_1 dT_2 dT_3}{T_{13}(T_{13}(1+\epsilon) + \delta)^2} \exp \left\{ -\frac{\delta(\mathbf{q}''T_3 + \mathbf{q}T_1 + \mathbf{q}'T_2)^2}{(1+\epsilon)T_{13}(T_{13}(1+\epsilon) + \delta)} \right\} \\
&\quad \exp \left\{ -\mu^2 T_{13} - \frac{T_1 T_3 (q - q'')^2 + T_1 T_2 (q - q')^2 + T_2 T_3 (q' - q'')^2}{T_1 + T_2 + T_3} \right\} \\
&\quad \exp \left\{ -\epsilon(\mathbf{q}^2 T_1 + \mathbf{q}'^2 T_2 + \mathbf{q}''^2 T_3) - \frac{\epsilon(\mathbf{q}T_1 + \mathbf{q}'T_2 + \mathbf{q}''T_3)^2}{(1+\epsilon)T_{13}} \right\} \quad (58)
\end{aligned}$$

We see explicitly that the  $\delta \rightarrow 0$  limit produces a log divergence which can be removed by a single subtraction. The counter-term that will accomplish this can be taken at first order to be

$$\begin{aligned}
Z^{3/2}\Gamma_{\text{C.T.}}^{(1)} &\equiv g(Z_1 - 1)^{(1)} = -\frac{g^3}{(4\pi)^3} \int_0^\infty \frac{dT_1 dT_2 dT_3}{T_{13}(T_{13}(1+\epsilon) + \delta)^2} e^{-\mu^2 T_{13}} \\
&= -\frac{g^3}{2(1+\epsilon)^2(4\pi)^3} \left[ I \left( \frac{\mu^2 \delta}{1+\epsilon} \right) \left( 1 + \frac{\mu^2 \delta}{1+\epsilon} \right) - 1 \right] \\
&\sim -\frac{g^3}{2(1+\epsilon)^2(4\pi)^3} \ln \frac{1+\epsilon}{\mu^2 \delta} \quad (59)
\end{aligned}$$

$$Z_1 = 1 - \frac{g^2}{2(1+\epsilon)^2(4\pi)^3} \ln \frac{1+\epsilon}{\mu^2 \delta} \quad (60)$$

We can now write the relation between renormalized and bare coupling

$$\begin{aligned}
g &= g_0 \frac{Z^{3/2}}{Z_1} \\
&= g_0 \left( 1 + \frac{g_0^2}{2(1+\epsilon)^2(4\pi)^3} \ln \frac{1+\epsilon}{\mu^2\delta} - \frac{3}{2} \frac{g_0^2}{6(1+\epsilon)^2(4\pi)^3} \ln \frac{1+\epsilon}{\mu^2\delta} \right) \\
&= g_0 \left( 1 + \frac{g_0^2}{256(1+\epsilon)^2\pi^3} \ln \frac{1+\epsilon}{\mu^2\delta} \right)
\end{aligned} \tag{61}$$

and the Callan-Symanzik beta function is

$$\beta(g) \equiv \mu \frac{dg}{d\mu} = -\frac{g^3}{128(1+\epsilon)^2\pi^3} + O(g^5). \tag{62}$$

For  $\epsilon = 0$  this is the known result for the beta function for *planar*  $\Phi^3$  field theory.

## 7 Conclusion: The Renormalized Worldsheet

In this article we have studied the renormalization procedure within the regularized setting provided by the lightcone worldsheet description of the sum of planar diagrams. We found that, in addition to counter-terms equivalent to mass, coupling, and wave function renormalization, two additional counter-terms must be introduced, parametrized by  $\alpha$  and  $\beta$  in the modified bare propagator (12). We now show how these additional counter-terms enter the worldsheet description.

Let us first describe how our regulator  $\delta$  modifies the worldsheet action. The path integrand acquires a factor  $e^{-\delta\mathbf{q}_i^2}$  for each internal boundary labeled by  $i$ . Because of Dirichlet conditions, we can associate each such factor with the point on the worldsheet where the boundary is created. Referring to the worldsheet lattice, such a point  $(i, j)$  is characterized by Ising spin variables  $s_i^j = +1$  and  $s_i^{j-1} = -1$  or  $P_i^j = 1$  and  $P_i^{j-1} = 0$ . Thus the regulator is incorporated by adding to the worldsheet action the term

$$S_{\text{reg}} = \delta \sum_{i,j} \mathbf{q}_i^{j2} P_i^j (1 - P_i^{j-1}). \tag{63}$$

Passing to the mixed  $x^+, p^+, \mathbf{p}$  representation,

$$\Delta_0 \rightarrow \frac{1}{2p^+} \exp \left\{ -T \frac{(1+\beta)(\mathbf{q} - \mathbf{q}')^2 + \mu_0^2 + \alpha(\mathbf{q}^2 + \mathbf{q}'^2)}{2p^+} \right\}. \tag{64}$$

we see that the  $\beta$  counter-term can be included in the worldsheet formalism as a simple scale factor multiplying the worldsheet action

$$\int_0^T d\tau \int_0^{p^+} d\sigma \left[ \frac{1}{2} \mathbf{q}'^2 - \mathbf{b}' \mathbf{c}' \right] \rightarrow (1+\beta) \int_0^T d\tau \int_0^{p^+} d\sigma \left[ \frac{1}{2} \mathbf{q}'^2 - \mathbf{b}' \mathbf{c}' \right]. \tag{65}$$

Physically it describes a renormalization of the scale of transverse coordinates compared to longitudinal coordinates, and can also be thought of as a difference of the speed of light in the transverse directions compared to the longitudinal direction. Since the regularization we use breaks the Lorentz symmetry between longitudinal and transverse directions, it is natural to expect artifacts in the interacting theory to affect the relative speed of light in these directions. So in order to end up with Lorentz symmetry we need to introduce an asymmetry in the bare propagator tuned to exactly cancel the asymmetry induced by ultraviolet divergences. From the point of view of the worldsheet this adjustment just corresponds to renormalization of the worldsheet fields, and it changes the structure of the worldsheet action very little.

The  $\alpha$  counter-term represents a more substantial modification of the worldsheet action. It is clearly partly a boundary term because it only involves  $\mathbf{q}, \mathbf{q}'$  the values of  $\mathbf{q}(\sigma, \tau)$  on the boundary of the propagator's



worldsheet. However, it is multiplied in the exponent by  $1/p^+$  which is a global property of the worldsheet. But this nonlocal feature is shared by the bare mass term and can be represented in a similar way, by modifying the ghost contribution to the action. Recall from [16] the identity

$$\int \prod_{i=1}^{M-1} \frac{dc_i db_i}{2\pi} \exp \left\{ (1+\beta) \frac{a}{m} \left[ \frac{b_1 c_1}{\eta} + \frac{b_{M-1} c_{M-1}}{\xi} + \sum_{i=1}^{M-2} (b_{i+1} - b_i)(c_{i+1} - c_i) \right] \right\} = \frac{M}{\eta \xi} \left( 1 + \frac{\eta + \xi - 2}{M} \right) \left( (1+\beta) \frac{a}{2\pi m} \right)^{M-1}. \quad (66)$$

For  $\eta = \xi = 1$  the left side of this equation is just the lattice definition for one time-slice and for one pair of ghost fields of the worldsheet path integral for the massless free scalar propagator. Therefore, including  $(D-2)/2 = d/2$  ghost pairs and  $N$  time-slices and calling the ghost action, for general  $\eta, \xi$ ,  $S_{\eta\xi}^g$ , we can write

$$\begin{aligned} (\eta\xi)^{Nd/2} \int D\mathbf{c}D\mathbf{b} e^{-S_{\eta\xi}^g} &= \left( 1 + \frac{\eta + \xi - 2}{M} \right)^{Nd/2} \int D\mathbf{c}D\mathbf{b} e^{-S^g} \\ &\sim \exp \left\{ -\frac{mTd}{2ap^+} (2 - \eta - \xi) \right\} \int D\mathbf{c}D\mathbf{b} e^{-S^g}. \end{aligned} \quad (67)$$

Comparing to (64), we see that the bare mass term and the  $\alpha$  counter-term will be produced if we choose  $\eta, \xi$  so that

$$\frac{md}{a} (2 - \eta - \xi) = \mu_0^2 + \alpha(\mathbf{q}^2 + \mathbf{q}'^2). \quad (68)$$

For example, we could choose

$$\eta(\mathbf{q}^2) = 1 - \frac{a}{md} (\mu_0^2 + \alpha \mathbf{q}^2); \quad \xi(\mathbf{q}'^2) = 1 - \frac{a}{md} \alpha \mathbf{q}'^2 \quad (69)$$

We see that the  $\alpha$  counter-term introduces a non-trivial coupling between the worldsheet ‘‘matter’’ fields and worldsheet ghost fields on the boundary. To be completely explicit, the term that must be added to the Lattice worldsheet action to account for the bare mass and  $\alpha$  counter-terms is

$$\begin{aligned} -S_{\mu\alpha} &= (1+\beta) \frac{a}{m} \sum_{ij} b_i^j c_i^j (1 - P_i^j) \left\{ \left( \eta(\mathbf{q}_{i-1}^{j2})^{-1} - 1 \right) P_{i-1}^j + \left( \xi(\mathbf{q}_{i+1}^{j2})^{-1} - 1 \right) P_{i+1}^j \right\} \\ &\quad + \sum_{ij} P_i^j \left\{ (1 - P_{i+1}^j) \ln \eta(\mathbf{q}_i^{j2}) + (1 - P_{i-1}^j) \ln \xi(\mathbf{q}_i^{j2}) \right\}. \end{aligned} \quad (70)$$

The ‘‘bare’’ worldsheet action didn’t show such a coupling. It is important to appreciate that in spite of this non-trivial modification the renormalized worldsheet system retains a local worldsheet dynamics.

In this article we have developed further the worldsheet model proposed in [4] to describe the sum of the planar diagrams of scalar  $\Phi^3$  theory. We have studied the ultraviolet divergence structure and have established the necessary refinements in the definition of the model to ensure that it reproduces to all orders the *renormalized* perturbation expansion for spacetime dimensions  $D \leq 6$ . We saw the need for new counter-terms parametrized by two new parameters  $\alpha, \beta$ . At tree level these parameters are zero but they must be tuned as a function of coupling and mass so that the renormalized perturbation theory is correctly reproduced. Unfortunately, we do not know *a priori* what values to choose for these new parameters.

Our refined worldsheet system is completely regulated and rigorously defined on a worldsheet lattice. On the lattice it enjoys a local worldsheet dynamics. One is therefore in a position to apply numerical methods for its solution. In such studies we must regard  $\mu_0, g_0, \alpha, \beta$  as adjustable parameters of a system that is not Lorentz invariant for generic values of these parameters. Thus one must be able to scan over different parameter sets and test for consistency with Lorentz invariance to help determine them.

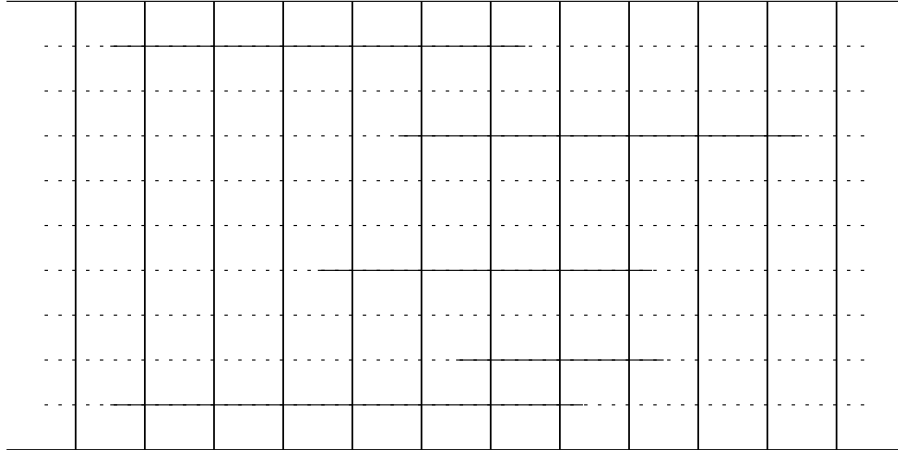


Figure 3: Lattice worldsheet for a multi-loop planar diagram. Time ( $\tau = ix^+ = ka$ ) flows left to right, and the vertical direction measures  $p^+ = Mm$ . The horizontal solid line segments show the location of the loops.

One promising numerical approach is Monte Carlo simulation. The worldsheet path integral for the  $q$  variables and the Ising spins clearly involves a positive definite integrand. The Grassmann  $bc$  variables, introduced to give a local description, clearly introduce minus signs and ensuing complications for Monte Carlo methods. On the other hand, if one integrates out the ghosts, positivity is again restored at the expense of some non-locality. Because the ghost dynamics is independent on each time slice, the relevant determinants are only one dimensional, and there is hope that their evaluation won't be prohibitively time consuming.

Our real interest in worldsheet methods is in tackling the large  $N_c$  (planar) limit of QCD, not planar  $\Phi^3$  scalar field theory. It is therefore an important next step to extend the analysis of this article to that case. The “bare” worldsheet system has already been constructed in [5]. We anticipate that the necessary counter-terms will be more numerous than for the scalar theory studied here, because of the gluon spin and issues with  $p^+ = 0$  divergences. We hope to resolve these difficulties in the near future.

Acknowledgments: I am grateful to K. Bardakci, S. Glazek, J. Klauder, and S. Shabanov for valuable discussions. I would also like to thank M. Shifman and M. Voloshin for their helpful criticism of this work. This research was supported in part by the Department of Energy under Grant No. DE-FG02-97ER-41029.

## A Appendix

The worldsheet for the general planar diagram, an example of which is depicted in Fig. 3, has an arbitrary number of horizontal solid lines marking the location of the internal boundaries corresponding to loops. Each interior link  $j, j - 1$  of a solid line at spatial location  $k$  requires a factor of  $\delta(\mathbf{q}_k^j - \mathbf{q}_k^{j-1})$ . To supply such factors, assign an Ising spin  $s_k^j = \pm 1$  to each site of the lattice. We assign  $+1$  if the site  $(k, j)$  is crossed by a vertical solid line,  $-1$  otherwise. We also use the spin up projector  $P_k^j = (1 + s_k^j)/2$ . We implement the Dirichlet conditions on boundaries using the Gaussian representation of the delta function:

$$\left(\frac{2\pi m}{a}\right)^{d/2} \delta(\mathbf{q}_i^j - \mathbf{q}_i^{j-1}) = \lim_{\epsilon \rightarrow 0} \frac{1}{\epsilon^{d/2}} \exp\left\{-\frac{a}{2m\epsilon}(\mathbf{q}_i^j - \mathbf{q}_i^{j-1})^2\right\}, \quad (71)$$

We keep  $\epsilon$  finite until the end of the calculation. Using this device, our formula for the sum of *bare* planar diagrams is [4, 16]:

$$\begin{aligned}
T_{fi} = & \lim_{\epsilon \rightarrow 0} \sum_{s_i^j = \pm 1} \int DcDbDq \exp \left\{ \ln \hat{g} \sum_{ij} \frac{1 - s_i^j s_i^{j-1}}{2} - \frac{d}{2} \ln(1 + \rho) \sum_{i,j} P_i^j \right\} \\
& \exp \left\{ -\frac{a}{2m} \sum_{i,j} (\mathbf{q}_{i+1}^j - \mathbf{q}_i^j)^2 - \frac{a}{2m\epsilon} \sum_{i,j} P_i^j P_i^{j-1} (\mathbf{q}_i^j - \mathbf{q}_i^{j-1})^2 \right\} \\
& \exp \left\{ \frac{a}{m} \sum_{i,j} \left[ A_{ij} \mathbf{b}_i^j \mathbf{c}_i^j - B_{ij} \mathbf{b}_i^j \mathbf{c}_i^j + C_{ij} (\mathbf{b}_{i+1}^j - \mathbf{b}_i^j) (\mathbf{c}_{i+1}^j - \mathbf{c}_i^j) - D_{ij} (\mathbf{b}_{i+1}^j - \mathbf{b}_i^j) (\mathbf{c}_{i+1}^j - \mathbf{c}_i^j) \right] \right\}
\end{aligned} \tag{72}$$

$$A_{ij} = \frac{1}{\epsilon} P_i^j P_i^{j-1} + P_i^{j+1} P_i^j - P_i^{j-1} P_i^j P_i^{j+1} + (1 - P_i^j) (P_{i+1}^j + P_{i-1}^j) + \rho (1 - P_i^j) P_{i-1}^{j-1} P_{i-1}^j \tag{73}$$

$$B_{ij} = (1 - P_i^j) \left( P_{i+1}^j P_{i+1}^{j+1} (1 - P_{i+1}^{j-1}) + P_{i-1}^j P_{i-1}^{j+1} (1 - P_{i-1}^{j-1}) + P_i^{j-1} P_i^{j-2} P_{i+1}^j \right) \tag{74}$$

$$C_{ij} = (1 - P_i^j) (1 - P_{i+1}^j) \tag{75}$$

$$D_{ij} = (1 - P_i^j) (1 - P_{i+1}^j) P_i^{j-1} P_i^{j-2} \tag{76}$$

The parameter  $\rho = \mu_0^2 a / (dm - \mu_0^2 a)$  provides a bare mass  $\mu_0$  for the gluon. The dimensionless coupling constant  $\hat{g}$  appearing in this formula is related to the conventional dimensionful bare coupling  $g_0$  by

$$\hat{g}^2 = \frac{g_0^2}{64\pi^3} \left[ \frac{m}{2\pi a} \right]^{(d-4)/2} \tag{77}$$

Where  $d = D - 2$  is the dimensionality of transverse space. The first exponent in (72) supplies a factor of  $\hat{g}$  whenever a boundary is created or destroyed. The second exponent includes the action  $S_q$  for the free propagator together with the exponent in the Gaussian representation of the delta function that enforces Dirichlet boundary conditions on the solid lines. The contents of this exponent go to the discretized action for the light-cone quantized string, if the quantity  $a^2 P_i^j P_i^{j-1} / m^2 \epsilon$  is replaced by  $1/T_0^2$ , with  $T_0$  the string rest tension. The third exponent incorporates the  $\epsilon$  dependent prefactor for that representation of the delta function as a term in the ghost Lagrangian. The remaining exponents contain  $S_g$  together with strategically placed spin projectors that arrange the proper boundary conditions on the Grassmann variables and supply appropriate  $1/p^+$  factors needed at the beginning or end of solid lines.

## References

- [1] J. M. Maldacena, *Adv. Theor. Math. Phys.* **2** (1998) 231-252, hep-th/9711200.
- [2] I. R. Klebanov and M. J. Strassler, *JHEP* **0008** (2000) 052 [arXiv:hep-th/0007191].
- [3] J. Polchinski and M. J. Strassler, arXiv:hep-th/0003136; *Phys. Rev. Lett.* **88** (2002) 031601 [arXiv:hep-th/0109174]; *JHEP* **0305** (2003) 012 [arXiv:hep-th/0209211].
- [4] K. Bardakci and C. B. Thorn, *Nucl. Phys.* **B626** (2002) 287, hep-th/0110301.
- [5] C. B. Thorn, *Nucl. Phys. B* **637** (2002) 272 [arXiv:hep-th/0203167].
- [6] S. Gudmundsson, C. B. Thorn, and T. A. Tran, *Nucl. Phys. B* **649** (2002) 3, [arXiv:hep-th/0209102].
- [7] D. Berenstein, J. M. Maldacena and H. Nastase, *JHEP* **0204** (2002) 013 [arXiv:hep-th/0202021].
- [8] E. Witten, "Perturbative gauge theory as a string theory in twistor space," arXiv:hep-th/0312171.

- [9] G. 't Hooft, *Nucl. Phys.* **B72** (1974) 461.
- [10] P. Goddard, J. Goldstone, C. Rebbi, and C. B. Thorn, *Nucl. Phys.* **B56** (1973) 109.
- [11] S. D. Glazek, *Phys. Rev. D* **60** (1999) 105030 [arXiv:hep-th/9904029]; *Phys. Rev. D* **63** (2001) 116006 [arXiv:hep-th/0012012]; *Phys. Rev. D* **66** (2002) 016001 [arXiv:hep-th/0204171]; arXiv:hep-th/0307064.
- [12] C. B. Thorn, “Fields in the language of string: Divergences and renormalization,” arXiv:hep-th/0311026.
- [13] K. Bardakci and C. B. Thorn, *Nucl. Phys. B* **661** (2003) 235, [arXiv:hep-th/0212254].
- [14] K. Bardakci, “Self consistent field method for planar  $\phi^3$  theory,” arXiv:hep-th/0308197.
- [15] R. Giles and C. B. Thorn, *Phys. Rev.* **D16** (1977) 366.
- [16] C. B. Thorn and T. A. Tran, *Nucl. Phys. B* **677** (2004) 289, arXiv:hep-th/0307203.